ELSEVIER

Coordination Chemistry Reviews
199 (2000) 55–87

COORDINATION CHEMISTRY REVIEWS

www.elsevier.com/locate/ccr

The investigation of structure of heavy metal clusters and polynuclear complexes in powder samples with the radial distribution function method

V.I. Korsunsky

Institute of Chemical Kinetics and Combustion, Novosibirsk 630090, Russia

Received 11 November 1998; accepted 1 April 1999

Contents

Abstract 55
1. Introduction 56
2. More exact information on the method 58
3. Some details of the experimental technique 62
4. Solution of specific structural problems for clusters and polynuclear complexes 63
   4.1 Binuclear clusters: simple cases of detection of metal–metal bonds 64
   4.2 Binuclear clusters: more detailed determination of the structure 66
   4.3 Small compact clusters and polynuclear complexes. 68
   4.4 Iridium sulfates. An example of detailed formalisation of the structural model for the RDF interpretation 70
   4.5 Complexes containing open quasilinear chains of heavy atoms in amorphous samples . . 75
   4.6 Three-dimensional noncrystalline polynuclear networks 78
   4.7 Complexes with relatively heavy atoms in ligands and heteronuclear clusters 81
5. Some general remarks in conclusion 84
References 86

Abstract

A method is discussed to obtain direct data on the structure of clusters and polynuclear complexes of heavy metals both in amorphous and polycrystalline powder samples using the radial distribution function (RDF) $G(r)$ of atoms obtained from an X-ray powder diffraction curve when an appropriate single crystal to determine the structure directly is inaccessible. The RDF is a spectrum of interatomic distances of a substance. The distances of each type

PII: S0010-8545(99)00171-X

produce a peak in an RDF which is located at r equal to their length. The distances between heavy metal atoms manifest themselves as strong peaks and can be readily identified. The peak position provides the metal–metal distance and its intensity is proportional to the number of this kind of distance in a cluster. These key data, together with a chemical and spectral information on ligands and a crystallographic experience in possible structures, allows one to imagine a trial model of the structure of a complex. The geometry and parameters of the model (the interatomic distances including those between metal and ligand atoms in addition to metal–metal ones and their numbers) are then tested by a quantitative comparison of the calculated model RDF with the experimental RDF in detail. This test is really direct for heavy metal complexes because only the contributions of few types of distances including heavy atoms are of main importance in RDF and these are the distances the determination of which is most important to distinguish different possible variants of a cluster structure. No spectral method gives so definite and direct data on the arrangement of heavy metal atoms, the feature which distinguishes first of all a cluster or a polynuclear structure from that of any other compound. So, the RDF method fills in this gap. The results for polynuclear complexes of different nature are discussed to give a clear and practical picture of the potential of the RDF method in the field.

Keywords: Polynuclear complexes; Clusters; Structure; Powder samples; Heavy atoms; Radial Distribution method

1. Introduction

In chemical practice, substances are often obtained only in the form of amorphous or polycrystalline powders the structures of which cannot be determined directly with the help of conventional techniques of single crystal or powder crystallography. Their characterisation is then limited mainly by spectral methods. For clusters and polynuclear complexes, however, such information is usually insufficient to understand the nature of a complex and often even to detect its formation in a reaction. No spectral method gives direct and unambiguous data on the mutual arrangement of metal atoms, the main feature that distinguishes the structure of a substance of this type from the one of any other compound.

This review deals with the application of the method of radial distribution function (RDF) of atoms obtained from an X-ray diffraction curve of a powder (amorphous or polycrystalline) [1–4] to fill in this gap in spectral information for heavy metal derivatives. The general idea of the activity is as follows. The RDF is the one-dimensional spectrum of interatomic distances of the substance. First of all, it allows one to measure directly some key distances between the heavy metal atoms and to estimate their numbers. Then, one can imagine the trial structural model of the complex, using in addition the chemical and spectral information, which often gives a rather detailed picture of the ligand nature, and the huge experience of crystallography concerning the possible types of structures. The subsequent accurate calculation of the RDF of the model and its detailed comparison with the experimental RDF allows one to test the set of interatomic distances of the trial

structure. This is the most direct way to verify the proposed structural model of the complex provided the coordinates of atoms (direct structure) cannot be measured.

The total RDF $D(r)$ of a substance can be represented as a superposition of partial $G^m_{kj}(r)$ peaks, each peak originating from some type of interatomic distance. Fig. 1 shows a simplified scheme of this superposition (the detailed analysis of the exact complicated form of $G^m_{kj}(r)$ is given in [5,6]). The subscripts k and j indicate atomic kinds, and the superscript m indicates a type of distance. For instance, $m=1$ may mark the distances between the metal atom (sort k) and the nearest oxygen atoms (sort j), $m=2$—the distances to some kind of more distant oxygens, etc. The peak $G^m_{kj}(r)$ is located at r equal to the mean value of a corresponding interatomic distance R^m_{kj}. Its width is determined by (1) the amplitude of thermal vibrations; (2) some possible diversity of the length of a distance of the type m (a structural disorder); (3) an apparatus broadening due to the procedure for obtaining the RDF [5,6]. An integral intensity I^m_{kj} of a peak $G^m_{kj}(r)$ is proportional to the number of corresponding distances N^m_{kj} per chosen stoichiometric unit of specimen to which the experimental RDF is normalized [1–4].

$$I^m_{kj} = w_{kj} N^m_{kj} \tag{1}$$

where w_{kj} is the weight of any distance between the atoms of sorts k and j. Relative weights of various types of distances in an RDF depend on the method used to obtain a diffraction curve (the scattering of X-rays, neutrons, electrons, the EXAFS spectra), a corresponding RDF being in all cases its Fourier transform.

Thus, the individual peak $G^m_{kj}(r)$ of an RDF contains in principle unique direct structural information on the interatomic distance R^m_{kj} and on the number of these distances N^m_{kj}. However, it is usually impossible to isolate such a peak with certainty due to its strong overlap with neighboring peaks. When distances of different type have close weights w_{kj}, each observed peak in an experimental RDF consists of several contributions $G^m_{kj}(r)$ of close intensities. The RDF interpretation is then very ambiguous and of little use in understanding the really interesting structures. On

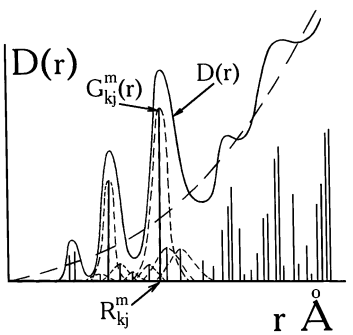

Fig. 1. The schematic view of an RDF. Solid line, a total RDF $D(r)$; vertical lines represent schematically positions R^m_{kj} and intensities I^m_{kj} of individual (partial) peaks $G^m_{kj}(r)$ produced by different types of interatomic distances; short dashes show the profiles of individual peaks; the parabola shown with the long dashes represents an average radial distribution of distances (see Section 2).

the contrary, if, as shown in Fig. 1, few types of most intense peaks $G_{kj}^{m}(r)$ corresponding to distances of the greatest weights w_{kj} determine in the main the form of the observed RDF, the problem of overlap is not so important in determining the parameters of those distances of the highest weight. If such distances are of principal importance to solve the structure, the RDF method will be really useful.

This is just the case for heavy metal clusters and polynuclear complexes, if the RDFs are obtained from powder X-ray diffraction curves. In such an RDF, the weight w_{kj} of an interatomic distance is approximately proportional to the product of the number of electrons in the atoms of a pair.

$$w_{kj} \sim Z_k Z_j \tag{2}$$

It is quite clear that a subsystem consisting of a few heavy metal atoms with high Z_k is much more noticeable in an RDF than a system with more numerous light ligand atoms. For instance, the weight of a distance between platinum atoms is $100 \div 150$ times larger than that of a distance between C, N, and O atoms. The distances between heavy metal atoms usually manifest themselves in the RDF as very strong peaks and can be readily identified. The position of such a peak at once gives an accurate first approximation for the metal–metal distance. The contribution of distances between light atoms produces only a background of low significance. The distances between heavy and light ligand atoms can, in principle, produce a rather noticeable contribution due to their intermediate individual weights w_{kj} when such distances are numerous, i.e. corresponding N_{kj}^{m} in Eq. (1) are high. Nevertheless, even in this case, as a rule the contributions of only one or two types of distances between heavy atoms in a cluster nucleus provide the main features of an intense RDF peak.

The RDF properties outlined above allows one to determine the key metal–metal distances in polynuclear complexes. The way to verify model structures by comparing the experimental and model distance spectra becomes really informative and convincing. One has in the RDF no complicated interference of many types of contributions of almost the same weight. Of importance are only those produced by a small number of types of interatomic distances which are, at the same time, most sensitive to the various structures of polynuclear species.

Few papers are known to us which have to any extent used a somewhat similar approach [7–10]. At the same time, we started in the mid-1980s to systematically study clusters and polynuclear complexes using the RDF method [11–13]. At present, the accumulated information allows us to demonstrate the real potential of the method for various cases.

2. More exact information on the method

The RDF method is rather old and well-known, in particular, in the areas of physics and physical chemistry of liquids and amorphous solids. The theory of the method is reported e.g. in the monographs [1–4]. We give here some relationships to help the reader to understand more accurately and in more detail both the above qualitative statement of the problem and the treatment and interpretation of experimental data.

The experimental RDF $G(r)$ is calculated by means of the numerical Fourier transformation of the structure-sensitive part of the X-ray scattering intensity curve $I(q)$ the so-called reduced intensity $qi(q)M(q)$ [1–4].

$$G(r) = (2r/\pi) \int_0^{q_{max}} qi(q)M(q) \sin(qr)dq \quad (3)$$

Here $q = 4\pi \sin\vartheta/\lambda$; ϑ is half of the scattering angle; λ is the radiation wavelength;

$$i(q) = \{K/[P(q)A(q)]\}I(q) - \sum_j n_j f_j^2(q) - I_{incoh}(q) \quad (4)$$

K is a normalizing constant which reduces $I(q)$ to absolute (electron) units; $P(q)$ and $A(q)$ are the polarisation and radiation absorption factors; Σ_j is a sum over all types of atoms in the stoichiometric unit of a substance to which $I(q)$ is normalized; n_j and f_j (q) are the number of j-type atoms in this unit and its atomic scattering amplitude; $I_{incoh}(q)$ is the intensity of incoherent (for X-rays Compton) scattering by the same stoichiometric unit. We have used the so-called modifying function $M(q)$ in the form

$$M(q) = [\sum_j n_j f_j(0)]^2/[\sum_j n_j f_j(q)]^2 \quad (5)$$

There exists no unified standard approach for the structural interpretation of an RDF in the literature. Various authors at various times used different techniques. We will briefly outline here the approach which seems to us most adequate and allows one to extract reliably direct structural information without exaggeration of the potential of the method. The formulae summarized below are available in one form or another in the literature devoted to the theory of the method.

To test the assumed structure, one has to compare the RDF of the model G_{mod} (r) with the experimental one. The computation of G_{mod} (r) includes a rather precise calculation of the contribution $G_{kj}^m(r)$ (peak shape and intensity) of each type of interatomic distance in the model. One obtains then G_{mod} (r) as the sum over all these distances determined by the pairs of types of atoms (k, j) and by the types of distances m within each pair. Thus,

$$G_{mod}(r) = -4\pi\rho_0 r^2[\sum_j n_j f_j(0)]^2 + \sum_{(k,j),m} G_{kj}^m(r) \quad (6)$$

$$G_{kj}^m(r) = (2r/\pi) \int_0^{q_{max}} qi_{kj}^m(q)M(q) \sin(qr)dq \quad (7)$$

$$qi_{kj}^m(q) = f_k(q)f_j(q)(N_{kj}^m/R_{kj}^m) \exp[-(\sigma_{kj}^2/2)q^2] \sin(R_{kj}^m q) \quad (8)$$

Here in Eq. (6), ρ_0 is the mean density of stoichiometric units (their number in Å^3). One calculates the integral (Eq. (7)) numerically with the upper limit q_{max} being the same as in Eq. (3) for the experimental RDF.

The latter formula (Eq. (8)) for a partial structure function $i_{kj}^m(q)$ is a version of the Debye formula [1–4] describing diffraction at a pair of atoms. It corresponds to the Gaussian distribution of an interatomic distance with a radial density $\rho_{kj}^m(r)$ of j-type atoms round k-type atoms given as

$$4\pi r\rho^{m}_{kj}(r) = [N^{m}_{kj}/(\sqrt{2\pi}\sigma^{m}_{kj}R^{m}_{kj})] \times \{\exp[-(r-R^{m}_{kj})^2/(2\sigma^{2}_{kj})] - \exp[-(r+R^{m}_{kj})^2/(2\sigma^{2}_{kj})]\} \quad (9)$$

This is a good approximation for intramolecular distances being primarily important when the RDFs of models are calculated. It guarantees the correct shape of $G_{mod}(r)$ peaks.

In all formulae, σ^{m}_{kj} is a root mean square deviation of the distance of the given type from its mean value R^{m}_{kj}, and N^{m}_{kj} is the number of these distances per stoichiometric unit. One has to include in N^{m}_{kj} the distances of (k,j)-type as well as of (j,k)-type taking as the first the atoms of both types. For example, one counts first all the Pt–Cl distances of length 2.3 Å around all the Pt atoms of the stoichiometric unit and then counts all Pt neighbors around each Cl atom of this stoichiometric unit. The atom of the second type in the pair may not belong to the chosen stoichiometric unit as is e.g. the case for bridging fragments. So, the formula to calculate finally N^{m}_{kj} is

$$N^{m}_{kj} = (2-\delta_{kj})n_k C^{m}_{kj} \quad (10)$$

where n_k is the number of the k-type atoms in a stoichiometric unit; $\delta_{kk}=1$, $\delta_{kj}=0$ if $k\neq j$; C^{m}_{kj} is the number of the j-type neighbors around the k-type atom at the distance R^{m}_{kj}. One chooses the type of the first atom k in Eq. (10) to have a more convenient way to count the neighbors. It is usually the metal atom in the model of the complex.

Eqs. (7) and (8) show that a peak $G^{m}_{kj}(r)$ is the stronger in the RDF the larger are the atomic scattering amplitudes $f_k(q)$ and $f_j(q)$ in the pair of atoms producing this peak. These formulae express more accurately the basic preference of an RDF obtained from X-ray scattering to study the structure of heavy metal clusters than the semi-quantitative Eqs. (1) and (2). The $f(q)$ of heavy atoms are several times larger for X-rays than those of light atoms. This is the largest difference among the methods mentioned above for obtaining the RDFs.

Eqs. 6–10 also show the parameters of a structural model necessary to calculate its RDF. They illustrate what features of the model structure one tests directly by comparing the model RDF with the experimental one. To calculate the RDF, the model has to be transformed into the sets of parameters N^{m}_{kj}, R^{m}_{kj} and σ^{m}_{kj}. The geometry of the model (the mutual arrangement of its atoms) gives the sets of N^{m}_{kj} and R^{m}_{kj}. One can somewhat vary R^{m}_{kj} within reasonable limits to achieve a better agreement with the experiment. This is the way to refine the initial approximations for interatomic distances. The model must be realistic and spatially realisable. So, varying R^{m}_{kj}, one should keep in mind the typical values of the bond lengths as well as of the valence angles to estimate accurately the distances between non-bonded atoms. It is also necessary to take into account the spatial limitations imposed by the model geometry and by possible approaches of non-bonded atoms. N^{m}_{kj} are rigid parameters for a given model and do not vary. If

one fails to fit the model RDF with the experimental one at a given set of N_{kj}^m, this means that the trial model is incorrect and has to be changed.

The most uncertain fitting parameters are σ_{kj}^m, the analogs of thermal parameters in single crystal X-ray analysis. When varying σ_{kj}^m, one should keep in mind their typical values which were determined by simulations of RDFs of various reference compounds of a known structure. Furthermore, the general restrictions are those: (1) the values of σ_{kj}^m for intramolecular distances must lie within the limits given by the reasonable amplitudes of atomic vibrations; and (2) σ_{kj}^m must be larger for distances between the atoms that are not connected through direct bonds than for those bonded through chemical bonds.

The model RDF can be quantitatively compared with the experimental one only in the region of a relatively small r. This is usually the region of $r \leq 3.5$–4 Å in which the RDFs of models will be shown in the following figures. The main contributions are made here by intracomplex interatomic distances, the lengths and the numbers of which are accurately determined by the model of molecular structure. Contributions of numerous intermolecular distances are substantial for larger r. A detailed model for packing the clusters either in the crystal or in the amorphous solid is necessary to specify such distances. Using the RDF data, the creation and verification of such a model is mostly either impossible or not unique. So, at large r, it is only possible to control the agreement of positions (and semi-quantitatively of the intensities) of well pronounced strong peaks of the experimental RDF and of the long distances between heavy atoms in the molecular structure being assumed.

The so-called difference RDFs $G(r)$ (3) are shown as a rule in the following figures. The sum of all the contributions of interatomic distances $G_{kj}^m(r)$ (the second term in Eq. (6)) gives one the total RDF $D(r)$ shown in Fig. 1. This form of an RDF includes the trivial effect of a rapid increase of a mean number of interatomic distances at large r. So, $D(r)$ oscillates around the rapidly growing parabola described by the absolute value of the first term in Eq. (6). $G(r)$ differs from $D(r)$ by subtraction of this parabola and therefore oscillates around the r axis. A zero line for the absolute intensities of peaks in a $G(r)$ picture is a descending parabola given by the first term in Eq. (6) and depicted with the long dashes in the figures.

Two extra measurements with a substance have to be carried out to calculate both its experimental RDF from a diffraction curve and a model RDF. The first one is the determination of the chemical composition of a substance, hence the numbers n_j of all atoms which determine its stoichiometric unit. These data are included in the formulae given above and also play the principal role in the procedure to normalise the diffraction curve to obtain the constant K in Eq. (4) [1–4,12]. The second measurement is the determination of the mean density of a powder to obtain, together with the results of the chemical analysis, the value of ρ_0 in the Eq. (6) and to fix by this procedure a zero line for model contributions in $G(r)$.

3. Some details of the experimental technique

The details of our procedure of a measurement and a treatment of a scattering curve are given in [12]. Here we pay attention to the principal distinctions from the conventional routine used to obtain powder X–ray pictures in the majority of powder diffractometers. The optimum conditions for the RDF technique are very different, and so a significant readjustment of an instrument is necessary. This influences the possibility to work with the RDF method in a laboratory having a diffractometer.

Fig. 2 shows our scheme for the measurement of an X-ray scattering curve. The sample (shown as the black circle) is a special thin-walled glass capillary (0.01 mm wall thickness, 0.7–1 mm diameter) containing the powder ground up in a mortar. The thin walls of a capillary make a negligibly small contribution to the scattering curve. The capillary is adjusted and fixed on the goniometer axis using a special holder. This scheme allows one (1) to use the minimum amount of a substance (about 20–30 mg); (2) to work rather conveniently with substances sensitive to air and moisture, if necessary; (3) to have a sample of a rather homogeneous density; and (4) to have a constant scattering volume over the entire range of the angle 2ϑ from 1° to 110–120°. It is difficult to make a standard flat sample large enough to exclude scattering by the specimen holder and be homogeneous at the same time. An inhomogeneity will lead to unpredictable distortions of the scattering curve in the standard reflection scheme with a changing scattering volume.

Mo–K_α radiation of the short wavelength ($\lambda = 0.7107$ Å) must be used instead of the Cu–K_α radiation ($\lambda = 1.54$ Å) usually exploited in powder diffractometers. It is then possible to increase q_{max} almost two times in Eq. (3) (from 8–9 to 15–16 $Å^{-1}$) for the calculation of Fourier-transform and thus to increase the RDF resolution [1–4]. The resolution of RDF peaks obtainable with Cu–K_α radiation is insufficient to analyse this RDF reliably. In addition, for heavy atom compounds and using Cu–K_α radiation, it is impossible to obtain the X-ray scattering curve suitable for the accurate RDF calculation due to very high absorption of the radiation by the sample. The Ag–K_α radiation ($\lambda = 0.5609$ Å) can be of use for extremely high absorbing samples, or such samples may be quantitatively diluted with a powder consisting of only light atoms [12].

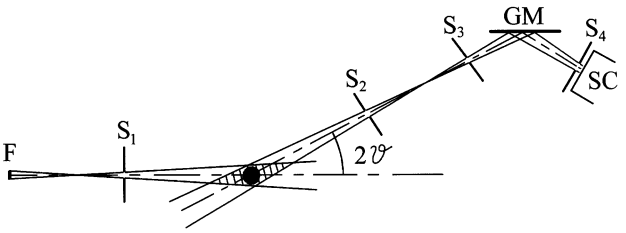

Fig. 2. The scheme for measurement of an X-ray scattering curve of a powder for the subsequent RDF calculation. *F* is a focus of an X-ray tube, S_1 is a primary beam slit, 2ϑ is a scattering angle, other notations are explained in the text (Section 3).

A crystal-monochromator (GM) must be located between the sample and the scintillation counter (SC) which in addition to its main purpose of monochromatizing the radiation remove the fluorescence of heavy atoms. In the RDF technique, the monochromator should mainly have the high transmission power necessary to measure the rather weak intensities particularly at large scattering angles. Therefore, one can employ here a simple flat graphite crystal-monochromator of relatively poor wavelength resolution and rather wide slits in front (S_3) and behind (S_4) the monochromator. For the RDF method, some worsening of the angular resolution due to the use of a relatively wide receiving slit S_3 is of no importance [12].

An additional slit S_2 (which is usually absent in the regular X-ray machine) should be on the goniometer between the sample and the receiving slit S_3. This slit restricts the irradiated volume visible to the counter (shaded) with dimensions slightly larger than the diameter of the capillary. This allows one to decrease the registered intensity of the scattering by air which is particularly noticeable at relatively small scattering angles.

4. Solution of specific structural problems for clusters and polynuclear complexes

In this Section, we consider examples of structural studies of clusters and polynuclear complexes of various nature starting from the simplest binuclear complexes and then proceeding to more complicated ones. Our aim is to demonstrate the potential of the RDF method for different cases, to show its various advantages and disadvantages. The author hopes that a reader will then be able to estimate independently the expediency to use the method to solve his own problems. As mentioned above, the model of a complex structure does not result from the RDF interpretation only. The model should actually be guessed using both key distances obtained from an RDF and a wider set of data obtained with the help of other methods, and thereafter the RDF allows this model to be tested directly in more detail. To imagine a model, it is especially important to determine the type of ligands and their roles in the complex which is sometimes possible using spectral methods and chemical experience. We cannot discuss this for each case in this review. We assume that the authors of the original papers have done their utmost in this respect. One should see the details in those papers. Some results will be demonstrated using compounds of known structure as examples. We have specially studied a lot of these substances to test the true potential of the method and to obtain experience in RDF interpretation. We give no complete sets of parameters of the models used in each RDF simulation shown in the figures. Only the most important are discussed. The detailed data are usually given in the original papers.

A short preliminary remark should be made about the structural drawings in the figures. They are not exact pictures of the commonly accepted whole molecular structures, when the X-ray single crystal analysis provides the coordinates for all the atoms. Here, as was emphasized above, only some specifically chosen interatomic distances can be directly determined from an RDF. Therefore, the structural

drawings represent in detail the arrangement of these chosen metal atoms as the main part of the model, and the structure of ligands is only often shown schematically. The metal atoms are designated as a rule with larger symbols than the light ligands atoms. The exact proportions of the bond lengths are sometimes not maintained to simplify the structural scheme. Owing to the limited space in the figures, some ligand atoms, whose locations are as a rule obvious, are not directly shown and some atomic groupings are designated with short symbols (Ph, CH_3, CF_3, NO_2 etc.).

4.1. Binuclear clusters: simple cases of detection of metal–metal bonds

The main structural sign of the metal–metal bond is a sufficiently short distance between the metal atoms. We will keep in mind this general geometric criterion and the typical commonly accepted values of the corresponding bond lengths when writing about bond detection with the RDF method. Of course, no information on the electronic structure of a compound can be obtained with the method, only the metal–metal distance.

Fig. 3 demonstrates a simple example of the direct detection of the Au–Au bond in bis-(triphenylphosphinegold)malonitrile in the RDF of its polycrystalline powder [12]. The picture of the known molecular structure of the cluster [14] is shown on the right. The first three peaks are actually of similar origin in most of the RDFs which will be demonstrated. All bonds between ligand atoms contribute to the common first peak near 1.5 Å. This peak is more or less pronounced depending on ligand type. The next peak normally appears near 2 Å or at somewhat greater r. Direct bonds between heavy metal atoms and the nearest light ligands atoms make contributions here. In this case, these are the Au–C ($R_{Au-C} = 2.1$ Å) and Au–P

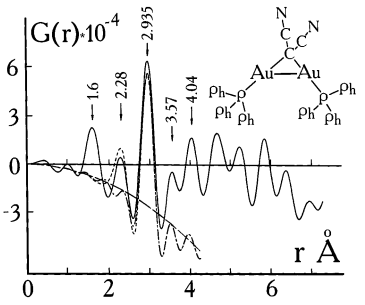

Fig. 3. $G(r)$ for bis-(triphenylphosphinegold)malonitrile. Here and in analogous figures: solid line is an experimental difference RDF; dashed-and-dotted line is a model contribution of distances between the heavy metal atoms (here Au–Au); short dashes show a sum of all contributions of near interatomic distances taken into account in a model RDF calculation (here AuAu + AuP + AuC); long dashes show a zero line for absolute intensities of peaks in $G(r)$ (see Section 2, the last paragraph). When the dashed-and-dotted and dashed lines coincide in any r-region in the RDF of a model, the common line in such a region is shown in the figures with the one of these types of dashes. A structure model is shown near the RDF which corresponds to the RDF simulation. Arrows indicate positions of maxima of peaks of an experimental $G(r)$. All $G(r)$ are given in e^2 $Å^{-1}$.

($R_{Au-P} = 2.28$ Å) bonds and the location of the peak maximum is determined by those with the heavier phosphorus atoms. Finally, the third, which as a rule is the strongest peak, contains the contribution of the nearest distances between the heavy metal atoms of a di- or polynuclear complex. Here, it is the distance Au–Au ($R_{Au-Au} = 2.93$ Å).

The model calculation indicates that the contribution of the single Au–Au distance in the molecule (dashes-and-dots) almost exhausts the intensity of the peak at $r = 2.935$ Å in the experimental RDF. A scarcely visible contribution is made to this peak by the few distances between Au atoms and the carbon atoms of CN-groups ($R_{Au-C} = 2.96$ Å). Here, the distance between the heavy metal atoms is manifested in a pure way as the strongest RDF peak.

This is often not the case however. Fig. 4a shows the RDF [12,13] of the cluster $Re_2(CO)_{10}$ of known structure [15]. The Re–Re distance (3.04 Å) in the carbonyl molecule only provides the major part (dashes-and-dots) of the intensity of the peak at $r = 3.085$ Å. The molecule contains ten Re···O distances of approximately 3.14 Å long, the distances being between Re atoms and oxygen atoms of the carbonyl groups. Their joint contribution is quite visible, though the weight $w_{Re\cdots O}$ of each Re···O distance is much smaller than $w_{Re\cdots Re}$ of the Re–Re one. Only the sum of the Re–Re and Re···O contributions (dashes) fits the intensity of the experimental peak. Its maximum is somewhat moved to the right of the Re–Re bond length due to the addition of Re···O.

Fig. 4b demonstrates a greater effect of masking the metal–metal bond by the Re–Cl bonds (2.33 Å) in the RDF of a polycrystalline powder of $(NH_4)_2[Re_2Cl_8]2H_2O$ [13]. The weight of the ReCl contact including semi-heavy Cl

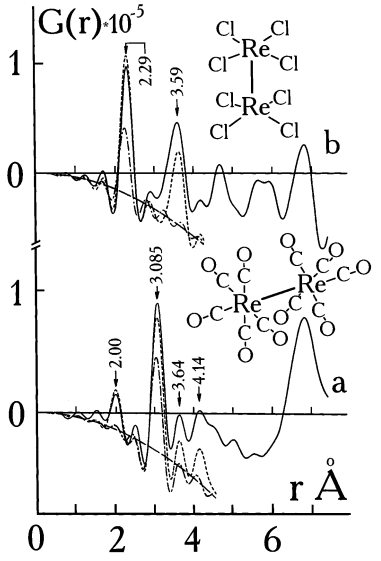

Fig. 4. $G(r)$ of $Re_2(CO)_{10}$ (a) and of $(NH_4)_2[Re_2Cl_8]2H_2O$ (b).

atom is approximately twice as large as that of the Re···O one. Therefore, the Re–Re bond (2.23 Å) [16] provides only half the intensity of the RDF peak at $r = 2.29$ Å. The rest is the contribution of the eight Re–Cl bonds. This is, of course, rather extreme. One or two Re–Cl bonds per Re–Re bond would not give such a significant side contribution. However, the possibility of an interference of this type predetermines the choice of objects to be studied with the RDF method. One should remove all unnecessary heavy and semi-heavy atoms that have no direct relation to the main problem which has to be solved. For instance, to detect a metal–metal bond, it is preferably to have a derivative containing (1) ligands consisting of the lightest atoms possible; and (2) light counter-ions if they are necessary. Br atoms are obviously less desirable than Cl atoms.

Usually, the metal–metal distance is sure to be discovered and measured within the accuracy of 0.02–0.03 Å [12,13] even in the presence of interfering contributions provided the latter are of reasonable quality and quantity. It imparts such high intensity to a peak that it cannot be exhausted with the contributions of distances of other possible types at a given stoichiometry of the substance and within the spatially realizable reasonable models of its structure. For instance, not more than half of the area under the peak at $r = 2.29$ Å in Fig. 4b could be filled in only with the contributions of all possible Re–Cl bonds. This directly confirms that the metal–metal contribution to the RDF is necessary without fail because no other explanation of its most intense peak is possible.

When one analyzes such an intense unresolved peak, one more problem may occur. Provided the experimental peak intensity is substantially greater than a model contribution of one metal–metal distance, one could in principle assume two possible explanations for an excessive part of the peak intensity. The first—contributions of numerous distances of metal–ligand type–has been discussed above. The second one is that the complex has a more complicated (than a binuclear) metal core and the additional intensity of the peak arises mainly from additional metal–metal distances (see Section 4.3). The choice between these possibilities depends in each case on the composition of a complex, on the type and the structure of ligands and their possible functions, on the data obtained with other methods, and on a detailed analysis of other RDF peaks based on a more complicated structural model, etc. For example, the contributions of the Re–Re type could fill in the peak at $r = 2.29$? in Fig. 4b, provided one assumes a model of a Re-chain or a small Re-cycle where each Re atom has two Re neighbors. However, no place for the contributions of the Re–Cl distances would remain under the peak, i.e. one should have to assume that there are no Re–Cl bonds in the substance. Since the latter is unreal in this case, the model of a binuclear complex remains the only one.

4.2. Binuclear clusters: more detailed determination of the structure

Some high intensity peaks, additional to those discussed above, can appear in an RDF and assist in determining the structure. The first two examples are given in Fig. 5. Here, the RDFs of polycrystalline powders of $(NH_4)_2[Re_2(HPO_4)_4(H_2O)_2]$ (a)

and $K_2[Pt_2(HPO_4)_4(H_2O)_2]$ (b) are shown [11,13,17]. The analysis of the RDFs has shown that both salts contain binuclear anions of the same structure as those in the analogous Cs salt for Re [18] and in the Na salt for Pt [19] phosphates of the known structure. The longer Pt–Pt bond (2.50 Å) gives the separate peak at $r = 2.51$ Å in the RDF (b) which is resolved from the peak of the nearest Pt–O distances at $r = 1.99$ Å. The shorter Re–Re bond (2.21 Å) gives the unresolved peak at $r = 2.18$ Å together with a minor contribution of the Re–O bonds (2.05 Å) in the RDF (a).

The symmetric arrangement of the four phosphate bridges at the metal–metal bond (Fig. 5) gives rise to a large number of almost equal distances of about 3 Å between the metal atoms and some of the ligand atoms. These are the Pt(Re)···P distances and the Pt(Re)···O distances to oxygen atoms coordinated by the neighboring Pt(Re) atom. In both cases, all these numerous distances contribute to the very strong joint peaks near $r \approx 3.1$ Å which do not overlap the peaks of the Re–Re and Pt–Pt distances. A characteristic picture of the RDF arises due to the appearance of a peak next to that of the metal–metal distance. Undoubtedly, it confirms the structure of the so-called 'lantern' type. In this case, the semi-heavy phosphorus atoms in the ligands favor the structural interpretation of the RDF because they increase the weight of the Pt(Re)···P distances sensitive to the ligand arrangement.

The determination of the analogous structure of the substance from the set of platinum(III) acetamidate complexes is probably one of the most impressive result of the employment of the RDF method. None of these compounds has previously been obtained in a single crystal form. The RDF of the polycrystalline powder and the model of the structure of the complex $[Pt_2(CH_3CONH)_4(NO_2)_2]$ [20] are shown in Fig. 6a. The shape of the RDF and the cluster structure are similar to those of the 'lantern' type Pt phosphate anion. Here, CH_3CONH-ligands produce the bridges instead of the phosphate groups in the previous case. The characteristic doublet is manifested in the RDF. Its first component at $r = 2.455$ Å corresponds to the strong Pt(III)–Pt(III) bond and the second one at $r = 3.025$ Å to the contributions of the Pt···O and Pt···C (instead of Pt···P in phosphate) distances.

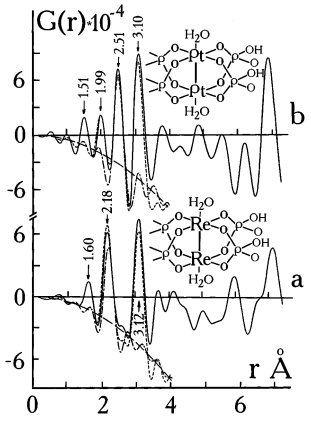

Fig. 5. $G(r)$ of $(NH_4)_2[Re_2(HPO_4)_4(H_2O)_2]$ (a) and of $K_2[Pt_2(HPO_4)_4(H_2O)_2]$ (b).

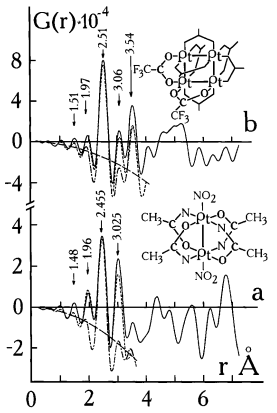

Fig. 6. $G(r)$ of $[Pt_2(CH_3CONH)_4(NO_2)_2]$ (a) and of $[Pt_4(CF_3COO)_8]$ (b).

Returning to Fig. 4b, the strong peak at $r = 3.59$? should also be mentioned here. It appears as a consequence of the special symmetric arrangement of Cl ligands in the binuclear anion $[Re_2Cl_8]^{2-}$. The numerous almost equal Re···Cl distances between directly non-bonded Re and Cl atoms contribute to this peak.

4.3. Small compact clusters and polynuclear complexes

In this section, the main objects are three- and four-nuclear complexes in which heavy atoms form compact rigid figures: an almost regular triangle, square, and tetrahedron. In such a structure, each metal atom has more than one heavy neighbor at a given metal–metal distance: two in a triangle and a square and three in a tetrahedron. According to Eqs. 6–10, a metal–metal distance peak must be two or three times stronger in the RDF of a compact cluster than that in the case of a binuclear complex, all RDFs being normalized on comparable stoichiometric units containing one heavy metal atom. This favors the application of the RDF method.

First, such a peak is easy to identify according to its typical high intensity. The substance could contain many more light atoms than is admissible in the case of a binuclear cluster, yet the strong metal–metal peak remains visible compared to the growing peaks of more and more numerous distances between light atoms (dilution of heavy atoms with the light atoms). In other words, it is easier to detect a polynuclear grouping than a binuclear one both in complexes containing large multiatomic ligands and in the background of admixtures. Second, the problem of obscuring contributions mentioned in Section 4.1 is not so important here. The number of distances between metal and ligand atoms which contribute to the same peak with the short metal–metal distances is usually not greater in a polynuclear complex (per metal atom) compared to a binuclear one. So, their interfering contributions look substantially smaller in comparison with the metal–metal distance contributions which have grown two or three times. This demonstrates the

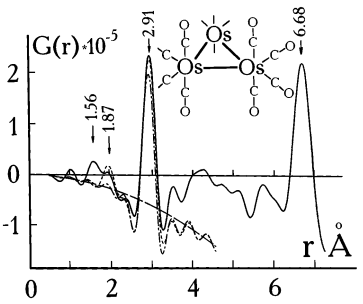

Fig. 7. $G(r)$ of $Os_3(CO)_{12}$.

comparison of the RDF [11,12] of the trinuclear [21] osmium carbonyl complex (Fig. 7) with that of the binuclear rhenium carbonyl complex (Fig. 4a). The contribution of Os–Os distances of 2.89 Å (dashes-and-dots) is almost sufficient to exhaust the area of the peak at $r = 2.91$ Å. The addition due to the Os···O distances is much less noticeable than the one in Fig. 4a due to the analogous Re···O contribution.

Fig. 6 demonstrates the transformation of the RDF upon transition from the binuclear platinum acetamidate (a) to the tetranuclear platinum trifluoracetate (b). In the latter, Pt atoms are found at the vertices of the square and two carboxyl bridges are located at each square side like the acetamidate bridges in the first compound (Struchkov and Batsanov, private communication). The Pt–Pt distance peak at the upper curve at $r = 2.51$ Å is two times larger compared to the corresponding peak at the lower one. At the same time, the number of Pt···O and Pt···C distances near 3 Å, typical of such bridges (see Section 4.2), is the same (counted per one Pt atom) as that in the binuclear acetamidate. Therefore, the peak of these distances at 3.06 Å in the RDF (b) remains of approximately the same intensity as the analogous one at 3.025 Å in the RDF (a) but does not look so strong with respect to the increased Pt–Pt peak. The additional noticeable peak in the RDF of the square cluster is the one at $r = 3.54$ Å produced by the Pt–Pt distance along the diagonal of the square Pt_4. Such a diagonal peak in RDF is an indispensable indication of any rigid figure (a square, a rectangle, a trapezium, etc.) formed by heavy atoms. It has been exploited by us in a series of studies [22–24].

Fig. 8 shows the RDFs of tetrahedral platinum complexes [22]. In both cases, the samples were the polycrystalline powders of potassium salts. Here, only the structures of tetranuclear anions are shown which determine the RDF shapes. The structure of the upper complex is known [25]. It is the mixed-valence complex $Pt_1(IV)Pt_3(II)$. The structure of the $Pt_4(IV)$ complex (bottom) was obtained as a result of our interpretation of the RDF (a) in [22]. The intensities of the very strong peaks at $r = 3.09$ and 3.13 Å correspond in both RDFs to three neighboring Pt atoms at approximately such distances near each Pt atom. The peak of the upper curve is slightly broadened due to a superposition of the contributions of the somewhat different distances Pt···Pt in the slightly distorted tetrahedron of the mixed-valence complex. The peak in the lower curve is narrower and corresponds

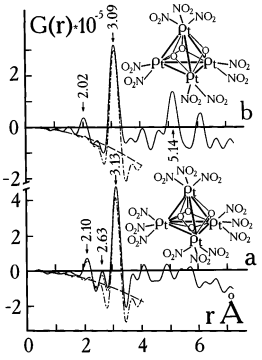

Fig. 8. $G(r)$ of $K_4[Pt_4O_4(NO_2)_{12}]4H_2O$ (a) and of $K_5[Pt_4O_3(NO_2)_9]3H_2O$ (b). The thick lines connecting Pt atoms in the model drawings does not mean here the metal–metal bonds, but only show the tetrahedra that are formed by the Pt atoms.

to the contributions of all equal Pt···Pt distances of 3.11 Å in the ideally symmetric tetrahedron. Here, the model of an isolated Pt_4 tetrahedron is confirmed by the total absence of any other pronounced RDF peaks up to $r > 8$ Å. This means that all Pt atoms, except the three nearest ones, are positioned far from any given Pt atom. So, a tetrahedron as an isolated species consisting of four equidistant Pt atoms remains the only possible arrangement of metal atoms in (a).

4.4. Iridium sulfates. An example of detailed formalisation of the structural model for the RDF interpretation

Using the results of our work [26], the procedure for a possible quantitative formalisation of a rather complicated model of the complex will be demonstrated. Such a formalisation is based on the direct estimation of the distance between metal atoms from the RDF supplemented with the obvious crystallographic experience and includes the fine details of the arrangement of ligands. First, this allows one to estimate the permissible interatomic distances which correspond to the spatially realisable structure and so to restrict the uncertainty of these parameters upon testing the model. Second, one can determine the details of the ligand arrangement by the RDF simulation with such a detailed model.

Fig. 9 shows the RDFs [26] of iridium nitridosulfate $(NH_4)_{10}[Ir_3(III,IV,IV)N(SO_4)_9]$ the analog of the known Delepine's salt [27,28] (b) and of the iridium oxosulfate $K_6H_4[Ir_3(III,III,IV)O(SO_4)_9]3H_2O$—one of the varieties of the Boisboudran's salt [29] (a). The structure shown of the nitridosulfate anion is similar to the one in the classical Delepine salt $(NH_4)_4[Ir_3(III,IV,IV)N(SO_4)_6(H_2O)_3]$ [28]. Three Ir atoms are placed at the vertices of an equilateral triangle. The μ_3-N atom bridging Ir atoms is found at the centre and two sulfate bridges are located at each side of the Ir_3 triangle. The labile H_2O ligands in the *trans*-position with respect to the central nitrogen in the Delepine salt are substituted in our sample by the additional sulfate groups. Unfortunately, the

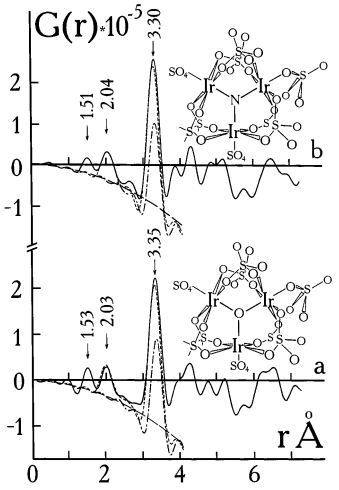

Fig. 9. $G(r)$ of $K_6H_4[Ir_3(III,III,IV)O(SO_4)_9]3H_2O$ (a) and of $(NH_4)_{10}[Ir_3(III,IV,IV)N(SO_4)_9]$ (b). The oxygen atoms of sulfate groups, that are located closer to the reader, are designated with the larger symbols than those located more far.

paper [28] is only a brief report containing the figure of the structure of the trinuclear anion and some bond lengths. The Ir···Ir distance, being of importance to us, is omitted. All quantitative parameters of the nitridosulfate structure given below were obtained by us in the course of the RDF (b) simulation [26].

The complex with a similar structure but with an μ_3-O atom at the centre was assumed long ago by various authors. However, there were no direct data due to the absence of a single crystal. After publication of our paper [26], the authors of [30] have obtained this as the mixed KCs salt. The results of the X-ray structure determination confirm the detailed structure of the trinuclear anion, found by us with the help of the RDF analysis [26].

The complete similarity of the RDFs of both compounds in the region of intracomplex distances up to $r \approx 3.7$ Å confirms the similarity of the anion structures. The Ir···Ir distances provide the principal contributions to the strong narrow peaks at $r = 3.35$ Å (a) and 3.30 Å (b). Therefore, their values can be estimated from the positions of the peak maxima to within several hundredths of Angstrom. However, in these structures, a lot of distances of the type Ir···O and Ir···S are of a length lying in the range of r under the same peaks. Their contributions give about half the peak intensities. Obviously, one should accurately take into account these distances to test the model. Also, one should not vary these distances independently because the parameters so obtained that allow one to describe the unresolved RDF peak may correspond to a spatially unrealisable structure, e.g. due to an inadmissible approach of valence non-bonded atoms. The qualitative scheme of the structure of the trinuclear complex should be formalized to estimate rather precisely all necessary distances.

A detailed analysis shows that only the central μ_3-N and μ_3-O atoms pull together the Ir atoms in the trinuclear complexes and keep them at the distances estimated from the RDFs (3.30–3.35 Å). Strictly speaking, this role of the μ_3-atoms is the main evidence for their existence in the structures because the contributions of either Ir–O or Ir–N bonds with the central atom can not be detected directly in the RDFs. They give only a small fraction of the intensities of the RDF peaks near 2 Å, the main contributions being from numerous other Ir–O bonds. On the contrary, the bridging SO_4 ligands push apart the metal atoms. Their arrangement requires noticeable distortion of the octahedral coordination of Ir atoms by turning back the equatorial Ir–O bonds out from the centre of the complex, provided the Ir···Ir distances are of the values mentioned above.

The other feature of the SO_4 bridges is that the bridging fragment OSO and the Ir···Ir line do not lie in the same plane which is achieved with a turn of the coordination octahedra of the Ir atoms through a substantial angle around the bonds with the central N or O atom. This remarkable detail of the structure is very different in the sulfate complexes than in the much more studied transition metal trinuclear complexes with double carboxylate bridges which are formally similar. The mentioned turn is either small or absent in the latter (see e.g. [31]). This difference is caused by the larger length of the S–O bond (approximately 1.5 Å) compared to the C–O bond in the carboxylate ion (approximately 1.25 Å).

The scheme of a double SO_4 bridge is shown in Fig. 10. It takes into account the qualitative conclusions discussed above and allows one to calculate all the necessary distances. One should consider only the arrangement of bridges on one side of the Ir triangle, keeping in mind the obvious symmetry of the model. The turn around the Ir bond with the centre of the complex is given by the value of the angle α measured from the position where the O_2 atom lies in the $X0Z$ plane and $\varphi = 90°$, i.e. when O_2 lies on the Ir_2A line. The degree of the turning back of the equatorial Ir–O bonds from the centre is specified with the excess of the angle φ over its ideal value of 90°.

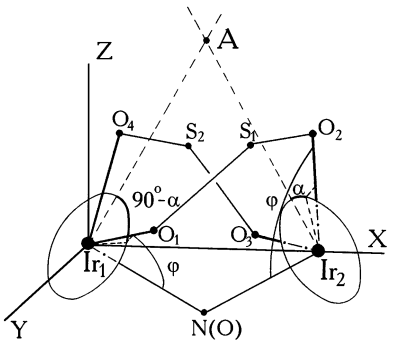

Fig. 10. The scheme for a double sulfate bridge at a side of the Ir triangle in the oxo- and nitridosulfates which specifies the computational parameters of the model described in the text (Section 4.4). The points A and N lie in the $X0Z$ plane.

The angles α and φ fix the configuration of the bridge and so the coordinates of atoms. They were determined by solving numerically the system of two trigonometric equations. The two equations represent the distances between oxygen atoms in the double bridge via (1) the Ir···Ir distance which is estimated from the strong RDF peak position; (2) the trivial length of Ir–O bond about 2 Å; and (3) the angles α and φ. The first equation is related to the $O_1 \cdots O_2$ distance inside the bridge. One can estimate it as 2.53 Å from the well-known rigid structure of the SO_4 tetrahedron. The second equation consists of the expression for the $O_2 \cdots O_4$ distance which is here equal to 2.8 Å, the minimum possible van-der-Waals approach of oxygens. Such a reasonable value can be achieved only due to the 'turning back' of the equatorial Ir–O bonds. The distance $O_2 \cdots O_4$ would be impossibly short at 2 Å without this distortion of the Ir coordination sphere, i.e. when $\varphi = 90°$ and provided the $O_1 \cdots O_2$ distance is equal to 2.53 Å and the Ir···Ir one to 3.35 Å.

For both compounds, $\alpha \approx 30°$ and $\varphi \approx 96.5°$ were determined. The $Ir_1 \cdots O_2$ distances of about 3.26 Å and of $Ir_2 \cdots O_1$ about 3.62 Å were estimated using these values of the angles. The position of a sulphur atom, e.g. of the S_1, was determined from symmetrical arrangement of a bridge, which means the equality of the angles $\angle Ir_1O_1S_1 = \angle Ir_2O_2S_1 = \gamma$. The value of $\gamma \approx 124.5°$ depends weakly on the value of the Ir···Ir distance, and therefore the Ir···S distances $\approx 3.15–3.20$ Å vary slowly when the Ir···Ir distance changes rather greatly.

All in such a way determined distances needed to be varied only to within 0.02–0.03 Å to fit the model RDF with the experimental one, i.e. obviously within the limits of the accuracy of their estimation. This guarantees the geometrical compatibility of the distances and their correspondence to the spatially realizable model. The finally determined Ir···Ir distances are for nitridosulfate 3.33 Å and for oxosulfate 3.38 Å. The results of the model simulation of the RDFs which agree well with the experimental functions are shown in Fig. 9. We have obtained the detailed structures of the trinuclear anions of both salts as a result of the RDF interpretation.

Experience gained upon the study of the computational model allows one to understand the further evolution of the trinuclear anion during oxidation to the Ir_3(IV,IV,IV) state [26]. Fig. 11 shows the corresponding RDF transformation. The single peak of the RDF of the Boisboudran's salt at $r = 3.35$ Å (the curve (a)) converts after oxidation into the well-resolved doublet with the maxima at 3.13 and 3.54 Å in the curve (b). The reconstruction of the doublet was performed in the framework of the same model but the Ir···Ir distances in the triangle became equal to 3.54 Å due to its expansion upon oxidation. These new Ir···Ir distances give the right-hand more intense component of the doublet. Calculations with this new Ir···Ir distance in the model have shown, that a decrease of the angle φ is mainly observed in the arrangement of the bridging SO_4 ligands ($\alpha = 29.5°$; $\varphi = 93.2°$), i.e. the distortion of the coordination octahedra of Ir atoms is decreased. The left-hand component give the Ir···S distances. First of all, these are the distances in the bridging fragments (3.15 Å) which are changed only slightly upon the increase of the Ir···Ir distance and also the distances to S atoms of SO_4 ligands in *trans*-posi-

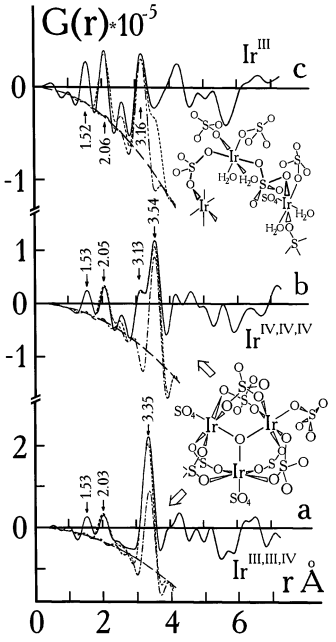

Fig. 11. The transformation of the RDF of Ir_3(III,III,IV) oxosulfate (a) upon oxidation (b) and reduction (c). In the upper RDF (c), the contribution of Ir···S distances is shown as the dashed-and-dotted line.

tions to the central oxygen (3.18 Å). The Ir···O distances produce contributions of a second order of magnitude. The shorter $Ir_1 \cdots O_2$ distances (3.33 Å) contribute between the doublet components, and the longer $Ir_2 \cdots O_1$ ones (3.71 Å) and those to O atoms of the *trans*-SO_4 groups (≈ 3.6 Å) contribute to its right-hand component.

The invariable topology of the trinuclear oxoanion agree with the reversibility of the redox transitions between the two forms described above [32]. On the contrary, the irreversible reduction of the oxosulfate Ir_3(III,III,IV) into a complex of Ir(III) leads to a decomposition of the trinuclear structure. This follows directly from the RDF (c) of the reduced product in which the strong Ir···Ir distances peak has vanished. The intensity of the peak at $r = 3.16$ Å is accounted for with contributions from only the Ir···S distances. This amorphous product is probably not a mononuclear sulfate of Ir(III) but contains disordered chains of Ir atoms coupled with single SO_4 bridges. The number of SO_4 ligands is insufficient to be independently coordinated by Ir atoms, and this follows from the composition of the specimen. However, in such a disordered chain, the distribution of Ir···Ir distances is very wide and they fail to form a narrow strong peak in the RDF.

Similarly using the same model to interpret the RDFs, we have obtained [33] the structures of two other trinuclear Ir sulfates. The first is analogous to Delepine's salt with the same set of degrees of oxidation Ir_3(III,IV,IV) but with O atom at the centre, and the second one is the trinuclear Ir_3(III,III,III) sulfate. The RDF and the structure of the first substance are fully similar to those shown in Fig. 9. The Ir···Ir

distance of 3.30 Å is even shorter than that in the nitridosulfate. The RDF of the second one is similar to the RDF (b) in Fig. 11 of the Ir_3(IV,IV,IV) form. However, the doublet of peaks at $r = 3.27$ Å and 3.81 Å is more prominent and shifted towards larger r. This doublet was interpreted by us as a manifestation of the same types of interatomic distances as above but in a more expanded triangle Ir_3(III,III,III), the Ir···Ir distance being of approximately 3.75–3.80 Å. The angle φ of approximately 90° corresponds to such a long Ir···Ir distance in the model. There is no distortion of the coordination octahedra and therefore sulfate bridges do not push apart Ir atoms. The O atom at the centre is not here obligatory to pull together the triangle. It is likely to be absent in this specially obtained complex. The trinuclear oxosulfate Ir_3(III,III,III) with an O atom at the centre is possibly unstable and therefore cannot be obtained by direct reduction of Boisboudran's salt.

The content of this Section illustrates with high clarity that it is important to estimate really the degree of ambiguity in a detailed test of a structural model with the simulation of an RDF. We do not imply the obvious limitation of the RDF method which does not allow one to distinguish between different models having similar or even identical sets of the principal interatomic distances. Even in the framework of a given model, one has to specify a rather large number of interatomic distances to simulate what is often a poorly resolved RDF. The calculations of such a type, involving a large number of parameters, could seem ambiguous in principle. However, the abundance of parameters is often only apparent. The set of substantial distances in an RDF reconstruction is determined actually by the distance between heavy metal atoms and by the limitations known from crystallography (the ligand structures, the typical bond lengths and valence angles, the possible approaches of valence non-bonded atoms, etc.). In the examples discussed above, the distance between the Ir atoms was the only nontrivial parameter, and it was directly fixed from the corresponding RDF. Thus, even a rather complicated model can be properly tested, if the above mentioned limitations are strictly followed.

4.5. Complexes containing open quasilinear chains of heavy atoms in amorphous samples

The detection and the study of this type of polynuclear objects have some peculiarities. In a rather long chain of metal atoms, each metal atom has two neighbors, and so, the peak of nearest metal–metal distances has a large integral intensity in RDF. This peak can be identified as easily as in RDFs of small cyclic clusters. Often, the model simulation of just this peak does not allow one to distinguish between the models of open and cyclic structures because, in both cases, the whole intensity of the peak corresponds mainly to the same number of metal–metal distances (two per one metal atom). Arguments in favor of one or another type of a metal skeleton of a complex may be found by analyzing in detail the peak shape, a spatial realizability of various models, data on ligands, etc. However, more direct evidence of an open structure can be obtained if explicit

peaks of distances between the second, third, etc. neighbors along the chain of heavy metal atoms are directly observed in an RDF.

Fig. 12 shows an impressive example of a such an RDF. This is the RDF of an amorphous platinum blue $[Pt_2(NH_3)_4(\mu\text{-}HPO_4)_2]_n$ which was isolated in the chain of redox transformations of *cis*-$[Pt(NH_3)_2(NO_2)_2]$ in concentrated H_3PO_4 [34]. The model of the blue's structure is shown next to the RDF, the arrangement of atoms being tested as usual with the reconstruction of the RDF peaks up to $r \approx 3.5$ Å [34]. The main structural unit in the model is the binuclear cluster with the direct Pt–Pt (2.65 Å) bond and two phosphate bridges in *cis*-position. The Pt–Pt bond makes the principal contribution to the peak at $r = 2.70$ Å, and the phosphate bridges give rise to the appearance of the peak at $r = 3.23$ Å in the same way as discussed in Section 4.2 for complexes of the lantern type.

These binuclear fragments form a rigid and almost colinear chain, the distance between their contacting Pt atoms being 2.8 Å. This distance contributes to the joint peak of nearest Pt–Pt distances at $r = 2.70$ Å. The subsequent distances between the heavy atoms along the chain (via one, two, etc.) are manifest as a sequence of equidistant sharp peaks at 5.47, 8.13, 10.87 Å. The step is approximately equal to the nearest mean distance Pt–Pt of about 2.7 Å. In this case, the nearest Pt–Pt separations of 2.65 and 2.8 Å are even shorter than those of 2.77 and 2.88 Å in the platinum blue with bridging α-pyridone ligands [35], the last distances being the shortest among the few similar 'blues' of known structure. This indicates a strong interaction of Pt atoms which can delocalize the electron density along the chain. The latter property seems to be typical of the blue Pt complexes with a fractional oxidation state of the metal [36].

Here, the chains of Pt atoms are noticeably longer than those of tetrameric platinum blues with large asymmetric organic ligands (α-pyridone, 1-methyluracil) which hinder the formation of longer chains [36]. The given phosphate blue is structurally closer to the octameric chain of Pt atoms consisting of dimers with double acetamidate bridges [37] which do not create such obstacles. In our case, the best fit of the RDF peaks in the $r < 3.5$ Å region is reached with the chain length of 6–8 Pt atoms (3–4 dimers). This was shown in [34] by varying the number of dimers in the chain thus changing the mean number of Pt–Pt separations of 2.8 Å

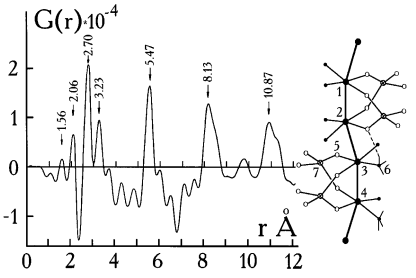

Fig. 12. $G(r)$ of the platinum blue $[Pt_2(NH_3)_4(\mu\text{-}HPO_4)_2]_n$. The various sorts of atoms are labelled with the help of numbers in the picture of the model: 1, 2, 3, 4 mark Pt atoms of the polymetallic chain; 5, an oxygen atom; 6, an ammonia ligand; 7, a phosphorus atom.

between the dimers in the model. The chain length thus obtained is probably some mean value, and the sample contains both longer and shorter oligomeric chains.

The manifestation of a comb of peaks of long distances between heavy atoms in a chain, as obvious as in the RDF in Fig. 12 and unambiguously interpretable, is possible only for amorphous samples. A disordered mutual arrangement of chains greatly broadens the distance distribution between Pt atoms of different chains. In contrast to polycrystalline samples, these distances do not manifest themselves as narrow strong RDF peaks additional to the ones produced by the sequence of rigidly fixed Pt···Pt distances along the rigid chain. So, one can observe the latter directly.

The results shown open the way to study with the RDF method many 'platinum blues' which are very often obtained as amorphous substances. However, this does not mean that any sample can be investigated successfully. It is necessary to perform chemical procedures to isolate the sample in which the blue is the main component rather than a coloring admixture.

Flexible polynuclear chains represent another extreme case where peaks from far distant heavy atoms are not explicitly manifested in RDF, though these chains are sure to exist in an amorphous sample. Distances between the nearest neighbors in a chain can be rigidly fixed by either bridges or direct interactions of metal atoms and so they give a strong narrow peak in an RDF as usual. However, the angle between such metal–metal bonds may have a wide distribution. As a result, the distribution of distances between heavy atoms via one or two sections along the chain will be broad. These distances will produce very broad peaks which do not stand out among other numerous contributions to an RDF tail and so are not observable explicitly. The nature of the amorphous state allows the existence of such disordered chains.

In [17,24,38], we have proposed chain structures of this type with bridging ligands. There, the chains are flexible due to various possible conformations of chain segments having different turns around some bonds in single bridges. This mechanism is similar to that realized in classical polymers. It is very difficult, if at all possible, to obtain single crystals for such compounds, which is also true for the major part of polymers. The RDF method gives one the way to directly confirm and to investigate the polynuclear structure of such objects. An example which deals with the detection and study of a flexible polymetallic chain consisting of gold atoms bonded through gold–gold interactions without bridging ligands [39] is given below.

In Fig. 13, curve (a) is the RDF of a bright-red amorphous modification of the compound 4-$NO_2C_6H_4NHAuPPh_3$ [39]. The doublet of strong peaks with the maxima at $r = 3.11$ and 3.42 Å reveals the existence of direct AuAu contacts. The intensities of the peaks correspond to the model where each Au atom has one neighbor at a distance of 3.07 Å and another one at 3.46 Å. So, there exist long chains of Au atoms as shown schematically in Fig. 13. The chain consists evidently of two different sections. The first one looks like a dimer with a rather strong Au–Au bond which corresponds to the former short separation. The other is formed with the longer and weaker interaction of Au atoms of the dimers. The

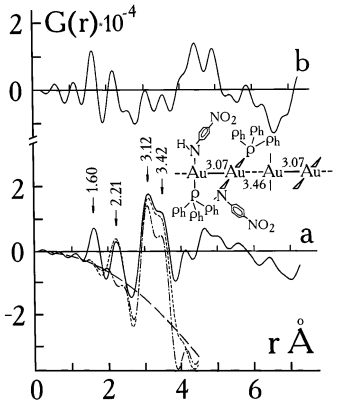

Fig. 13. $G(r)$ of the amorphous polynuclear bright-red (a) and of the mononuclear crystalline yellow (b) modifications of 4-$NO_2C_6H_4NHAuPPh_3$. The model structure of the former is shown.

latter interaction may not be so strongly directed as the former and makes a large disordering of the angles between the Au–Au bonds in the chain possible. Only smooth oscillations, typical of amorphous samples, are observed in the RDF in the region of $r > 4$ Å which suggests this type of disorder.

In this case, we have direct experimental justification of the fact that the above mentioned strong peaks in the curve (a) originate from AuAu contacts. The same compound has a crystalline yellow modification of known structure [40] in which the Au atoms are positioned far from each other. The RDF of a polycrystalline powder of this phase shows the curve (b) in Fig. 13. It contains no strong peaks near 3 Å typical of Au–Au bonds. Here, one has a curious example where metal–metal interactions are realized in a kinetically preferred *meta*-stable amorphous phase under the conditions of fast precipitation of a substance from a solution, while a stable crystalline phase with no metal–metal contacts is formed under conditions of slow precipitation [39,40].

4.6. Three-dimensional noncrystalline polynuclear networks

We imply here a rather spatially-extended polynuclear formation in which metal atoms are connected on the average with more than two neighboring ones. Owing to this, the chains of metal atoms branch off at a majority of metal centres of a polynuclear complex and this results in a network structure. The local structure of small regions of such a network may be close to or even coincide with the structure of any crystal. However, the structural defects and the irregularities of the ways of a network branching give rise to amorphous rather than crystalline substances.

Among the objects which we studied with the RDF method, samples of amorphous rhodium chloride [41] and of an amorphous product of high-temperature alkaline hydrolysis of the complex $[Rh(NH_3)_5Cl]Cl_2$ [42] can be attributed to this class. The former has the composition $RhCl_{(3+x)}(H_2O)_yH_x$ always with a higher Cl-ion content compared to crystalline $RhCl_3$. The formula of the second one is

$Rh(OH)_3(NH_3)_x(H_2O)_y$ ($0.5 < x < 0.8$ and $1.2 < y < 1.8$) and ammonia is involved in the rhodium coordination sphere [42] along with the OH ligands. The structure of both substances is similar. Here, we discuss in detail the second product since it contains the lighter ligands, and so the Rh···Rh distance contribution is more prominent in its RDF.

Fig. 14 shows the RDF of the sample of composition $Rh(OH)_3(NH_3)_{0.6}(H_2O)_{1.5}$. The first peak at $r = 2.06$ Å corresponds to the distances for up to six nearest OH and NH_3 ligands in the standard coordination Rh(III) octahedron. The second strongest peak at $r = 3.07$ Å corresponds to the distance between the nearest Rh atoms. The Rh···Rh distance of 3.07 Å may correspond only to the connection of neighboring coordination octahedra with the help of two bridging OH-groups at the common edge. So, this is the principal fashion of bonding in the polynuclear complex. The alternative possibilities, either with three OH-bridges at a common face or with one OH-bridge at a common vertex of octahedra, should give rise to Rh···Rh distances of near 2.4 and 4.1 Å, respectively. The bonding through vertices of a common edge also explains the origin of the next two RDF peaks at 3.63 and 4.79 Å. They are produced by the distances between a given Rh atom and atoms of ligands located in more removed vertices of octahedra of neighboring metal atoms. The model reconstruction of the intensity of the peak at $r = 3.07$ Å shows that each Rh atom has slightly less than three (2.7–2.8) neighboring Rh atoms at this distance. Thus, the main repeating structural element of the polynuclear complex is the set of four connected coordination octahedra, denoted by numbers 1, …, 4, Rh atoms being located at their centres. The RDF peak at $r = 5.32$ Å corresponds then to the distances between the Rh atoms inside the octahedra e.g. of types 2 and 3.

The regular repetition of this structural element around each octahedron would lead to the formation of an infinite flat layer whose fragment is shown in Fig. 14. Such layers are realized in e.g. the structure of the $RhCl_3$ crystal [43] with Cl atoms bridging octahedra. The amorphous sample with loss of long range order can arise due to irregularities of linkage between the octahedra. For instance, at some sites of the network, octahedra may join a given one through such edges that they leave the flat layer. Also, bonding is occasionally possible without branching of the ···Rh···Rh···Rh··· sequence. This occurs when a given octahedron connects only two neighboring ones by means of its opposite edges so that a third octahedron cannot

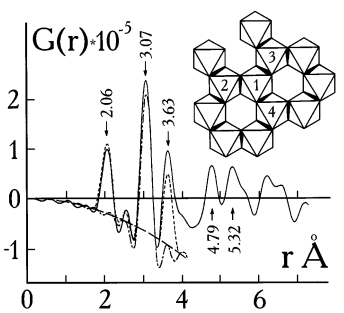

Fig. 14. $G(r)$ of $Rh(OH)_3(NH_3)_{0.6}(H_2O)_{1.5}$.

join the central one at all. The linkage through single vertices is also possible as an irregularity at some rare sites.

The possible existence of the last two types of packing defects is consistent with both the stoichiometry of the complex, different from the ideal $Rh(OH)_3$, and the number of neighboring Rh at each Rh atom less than three on average. The extra NH_3 and H_2O ligands could occupy non-bridging vertices of coordination octahedra of Rh which arise due to bonding defects. However, both these just mentioned experimental facts are most likely related mainly to a limited size of regions of more or less regularly OH-connected Rh octahedra. Each octahedron is connected, as a rule, with three similar ones in the inner part of such a finite cluster. On its surface, each octahedron is bonded to one or two octahedra from the inner region and the extra NH_3 and H_2O ligands as well as a part of OH-groups serve as the surface ligands. The strong X-ray scattering in relatively small angles ($2\vartheta \leq 5°$, Mo–K_α-radiation) directly confirms the existence of both the regions of a more dense packing of atoms in the inner ordered part of a cluster and regions of a smaller density formed by a disordered linking of cluster surfaces.

All this also holds for the structure of amorphous rhodium chloride with obvious corrections concerning the ligand types [41]. Its RDF is similar to the one just discussed, if one takes into account (1) the scaling along the *r* axis due to the longer Rh–Cl bond compared to the Rh–O one and (2) the redistribution of relative intensities of peaks in favor of those of metal–ligand distances due to the more heavier Cl ligands.

The high solubility of rhodium chloride in water allows one to observe readily and directly its depolymerization in solution. Fig. 15 shows the change of form of the scattering curve of a solution in the small angle region [41]. A strong small angle scattering is observed just after the dissolution of the salt due to a conservation in solution of large clusters, consisting of Rh and Cl atoms, which have higher average electron density compared to the surrounding water. However the small-angle scattering decreases rapidly during the first 4–5 h after dissolution. This indicates destruction of the clusters due to cleavage of Cl-bridges and water entering into the

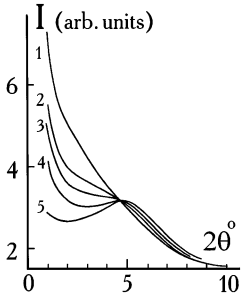

Fig. 15. The time dependence of small angle X-ray scattering of the water solution of amorphous rhodium chloride. The concentration of Rh is 2 g-ions l^{-1}. The time from dissolution up to the beginning of the measurement of the curve is for 1–20 min; 2–54 min; 3–95 min; 4–4.5 h; 5–7 days. The time for measuring one curve is ca 20 min.

Rh coordination sphere. In several days, the peak with a maximum at $2\vartheta = 5°$ typical of concentrated electrolyte solutions [44] is stabilized in the diffraction curve. This peak is related to the X-ray scattering on a packing of small complexes in a solution which here are most probably monomeric of the type $[RhCl_n(H_2O)_m]$ with their hydrate shells.

The example discussed shows that study of the time dependence of a small-angle scattering intensity may provide a general direct method to determine the stability of large polynuclear species in solution. A high intensity small angle scattering is unambiguously connected with the existence of such species having a mean electron density differing from that of the environment. Heavy multi-electron atoms in a polynuclear complex increase this contrast, i.e. provide a high sensitivity for this method.

4.7. Complexes with relatively heavy atoms in ligands and heteronuclear clusters

For objects of this type, it is possible to measure directly (1) distances between metal atom and heavy atoms in ligands and (2) sometimes distances between heavy ligands. This may be useful when the determination of an arrangement of ligands is one of the main questions to be solved. Of course, the substance should contain a reasonable number of heavy ligands, in order to have an RDF not too complicated and still interpretable. Here we describe in brief two examples [45,46].

The mixed-valence platinum complexes *cis*-$[Pt(II)(NH_3)_2(SCN)_2][Pt(IV)(NH_3)_2(SCN)_2I_2]$ **I** and $[Pt(II)(en)_2(SCN)_2][Pt(IV)(en)_2(SCN)_2I_2]$ **II** (en-ethylenediamine) were studied [45]. Their structures were assumed to be of the type depicted in Fig. 16 (structure b for **II** and c for **I**), on the basis of spectroscopic data and analogies of these data with those for compounds of known structure. Octahedral Pt(IV) and square-planar Pt(II) complexes alternate along the linear chains ···I–Pt(IV)–I···Pt(II)···I–Pt(IV)–I···Pt(II)···I–. An interaction between I and Pt(II) atoms delocalizes electron density along the chain. The RDFs have been obtained for polycrystalline powders of these compounds (Fig. 17), and both types of Pt(IV)–I and Pt(II)···I distances were directly detected and measured. For comparison, Figs. 16 and 17 show the RDF and the structure (denoted as a) of the reference substance $[Pt(II)(en)_2][Pt(IV)(en)_2I_2](ClO_4)_4$ **III** of known structure similar to that assumed for **I** and **II**.

All three RDFs have strong peaks at $r = 2.69–2.71$ Å corresponding to Pt(IV)–I bond contributions of typical length. The Pt(II)···I distances provide the main contribution to the intensities of peaks at 3.11 Å (a); 3.22 Å (b); and 3.55 Å (c). The whole model contribution of these two type distances are shown here with the dashed-and-dotted lines. The Pt(IV)–I distances are practically the same in all three substances but Pt(II)···I increases strongly from **III** to **I**. It is 3.10 Å in **III**, 3.23 Å in **II**, and 3.50 Å in **I** according to the RDF simulations. The interaction between complexes of Pt(II) and Pt(IV) and so the delocalization of electrons over the chain decreases in the same sequence. This influences the physical and spectral properties of the compounds: **I** is much closer to the pure mixed-valence complex Pt(II)Pt(IV),

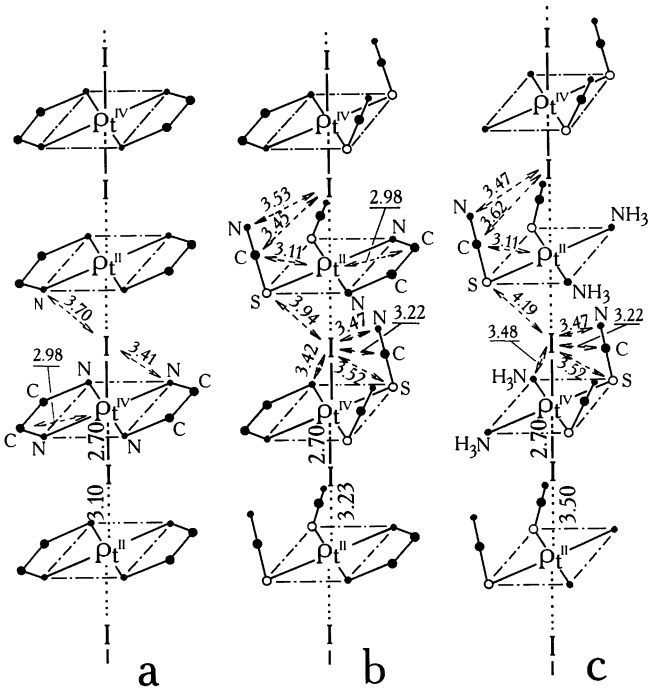

Fig. 16. The arrangement of Pt(II) and Pt(IV) complexes in one-dimensional chains in crystals of the substances **I** (c), **II** (b), and **III** (a) (Section 4.7). The values of interatomic distances are specified which are important for the simulation of the RDFs in the Fig. 17.

whereas in **II** and **III**, the platinum oxidation state is shifted towards an intermediate state Pt(III).

The RDFs in Fig. 17 also provide additional evidence of a practically colinear arrangement of heavy atoms in the chains. The strong peaks appear in all three curves at positions which coincide, within good accuracy, with the sum of the lengths of the corresponding distances Pt(IV)–I and Pt(II)···I. These are the peaks at $r = 5.73$ Å (a), 5.96 Å (b) and 6.08 Å (c). They probably correspond to the distances between the successive Pt(II) and Pt(IV) atoms, and the peak positions shift towards larger r in agreement with increase of the Pt(II)···I distance.

Measurement of the distances between the heavy ligands illustrates the study of a heteronuclear anion platinum–tin complex with citrate ligands $[(SnCitr)_4Pt(\mu\text{-}SnCitr)_2Pt(SnCitr)_4]^{6-}$ **IV** ($Citr^{3-} = {}^{-}OOC–CH_2–C(OH)(COO^{-})–CH_2–COO^{-}$) [46]. The RDF of its potassium salt (an amorphous substance) is shown in Fig. 18. The strongest peak at $r = 2.58$ Å corresponds to five or six Pt–Sn bonds at each Pt atom. The bond length of 2.58 Å is close to those of 2.55–2.57 Å in the known complex anion $[Pt(SnCl_3)_5]^{3-}$ **V** [47]. In the last compound, five Sn atoms are located at the vertices of a trigonal bipyramid around the central Pt atom. It was natural to assume at first that the structure of the platinum–tin core of the complex **IV** is the same since one of the methods of its synthesis was the substitution of

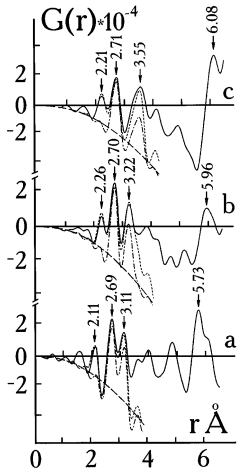

Fig. 17. G(r) of the substances **I** (c), **II** (b), and **III** (a) (Section 4.7). Here, the contributions of distances between Pt and I atoms are shown with the dashed-and-dotted lines.

Cl-ions in the periphery of **V** with citrate ions. However, this assumption is contrary to the RDF in the $r = 3.3$–4 Å region in which the main contribution is made by the distances between the heavy Sn atoms of the ligands. This contradiction is illustrated in the inset in Fig. 18. The dashed line of the model RDF and the solid line of the experimental one differ strongly in the given r-range.

Fig. 19 shows the model which allows one to reconstruct the RDF correctly as demonstrated in the main part of Fig. 18. Tin atoms are located at the vertices of a somewhat distorted octahedron around the Pt atom, and two of them are bridging in accordance with the stoichiometry of the complex **IV**. Citrate ligands are coordinated by all Sn atoms in the periphery of the complex anion. Sn-bridges connect two platinum–tin octahedra through a common edge. The Pt···Pt distance

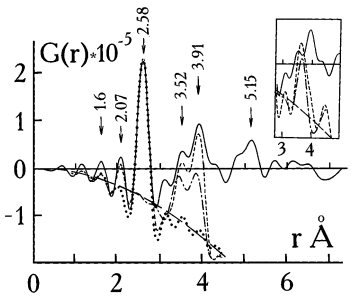

Fig. 18. $G(r)$ of the platinum–tin complex **IV** (Section 4.7). The RDF simulation shown in the main part of the figure corresponds to the model shown in the Fig. 19. Here, the model contribution of Pt–Sn bonds is shown with the large dots, and that of the distances between Sn atoms—with the dashed-and-dotted curve. The inset shows comparison of the RDF in the 3–5 Å r-region with the model simulation based on the trigonal–bipyramidal arrangement of Sn atoms around Pt atom described in Section 4.7.

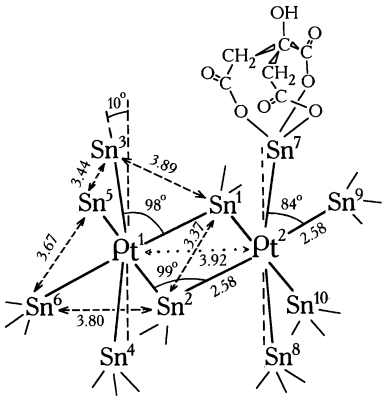

Fig. 19. The model of the structure of the platinum–tin complex anion **IV**. The interatomic distances and some bond angles are specified which are most important for the simulation of the RDF in the Fig. 18. The most probable way for coordinating a *citrate* ligand is shown at one of the Sn atoms. The other Sn atoms are assumed to be coordinated in a similar fashion.

near 3.9 Å in the binuclear complex gives a substantial contribution to the RDF peak at $r = 3.91$ Å. The octahedral coordination of tin atoms increases the number of Sn···Sn distances in the $r < 4$ Å region (all edges of the octahedron of 3.65 Å) compared to the bipyramid model in which the contributions of only the short edges of the same length of a bipyramid are not enough evidently to fill in the area under the RDF peaks (see inset in Fig. 18). The angle distortion between Pt–Sn bonds shown in Fig. 19 produces a diversity of Sn···Sn distances necessary to account for the splitting of the common peak of their contributions (dashed-and-dotted line in the model RDF). Such distortion is caused by the pushing apart of the large citrate ligands at the axial tin atoms ($Sn_{3,4,7,8}$). The model suggested also explains the origin of the last pronounced RDF peak near $r = 5.15$ Å, whose position corresponds to the doubled Pt–Sn distance. This peak is produced by numerous rigidly fixed intramolecular distances between Sn atoms in the opposite vertices of the octahedra.

This example illustrates a somewhat special case among all the others discussed above. The correct reproduction of the spectrum of distances between the heavy atoms of ligands (Sn) is decisive to choose the model of the complex structure. The main RDF peak which corresponds to Pt–Sn distances could be fitted within experimental accuracy to both the models discussed. The difference between the number of Pt–Sn distances (5 and 6) is not too large, and its influence on the model peak intensity can be compensated to a considerable extent with some reasonable variation of the parameter σ_{Pt-Sn} upon the RDF fitting procedure.

5. Some general remarks in conclusion

1. The RDF method, used with a clear understanding of its potential, allows one to obtain rather detailed structural information on substances which often either

remain beyond the limits of an investigation as intractable products or their characterisation is limited to indirect methods. These substances may be products of complicated reactions, intermediate products, complexes with complicated ligands, insoluble polymers, etc. It is often difficult to isolate such a substance in a pure form and moreover as a single crystal. At least, one could obtain with the RDF method stimulating information to justify further efforts to characterize such a substance more accurately and unambiguously. On the other hand, using RDF, the fate of a metal–metal bond could be directly followed up in a reaction even if the whole determination of the structure of a product is impossible.

2. We have not discussed the problem of studying polynuclear complexes in solution by means of the RDF technique. The main ideas of such a study coincide with those of a study of powders. However, the RDF method needs sufficiently concentrated solutions, clusters to make a leading contribution to an RDF, compared to that of the solvent. The low solubility of many clusters prevent structural investigation in solution. No detailed data are available now on the concentrations that are sufficient to study clusters. In articles [9,46], the metal–metal distance peaks have been readily observed when the concentration of heavy Pt or Os atoms were about 0.1–0.15 mol l^{-1}. Probably, these values should be quite different for various types of complexes.
3. The RDF method is now well-forgotten by chemists. One now applies the much more popular and well-known EXAFS method to try to solve problems like those discussed. However, in the EXAFS method, peaks of distances between metal atoms have intensities of a second order magnitude compared to main peaks of distances between a metal atom and nearest ligand atoms. The former are often unobservable, especially if the distances are longer than ≈ 3 Å. Special conditions are necessary to make metal–metal peaks detectable, e.g. either a very low temperature or a special type of a complex structure. No such limitations occur for the RDFs obtained from X-ray diffraction.

   The RDF method requiring a normal powder diffractometer is in principle experimentally more accessible. The RDF theory does not deal with the complications and approximations characteristic of the EXAFS theory. The physical nature of X-ray diffraction, which is the basis of the RDF method, is much simpler than the physical foundations of the EXAFS method. Thus the measured experimental data are more directly related to structure in the RDF technique. Of course, the RDF method has its own limitations and can not be used to solve many problems for which the EXAFS method provides valuable information, e.g. for diluted systems. However, the RDF method is preferable in the areas outlined above.
4. There is a rather narrow window in r values approximately from 2 to 3.5–4 Å in which one can really obtain quantitative information about the structure from an RDF. However, for heavy metal polynuclear complexes, the most important interatomic distances can be determined here directly in such an

obvious way, that one could compare this with the 'seeing' of these structural features. At the same time, the scanty information on metal atom arrangement obtainable with the majority of those spectral methods which are usually employed in the course of powder investigations could be classified probably only as the not very clear 'hearing' of something about the cluster nucleus structure. As the Russian proverb goes 'It is better to see once than to hear a hundred times'.

References

[1] A. Gunier, Theorie et technique de la radiocristallographie, Dunon, Paris, 1956, chs. 5 and 11. (Russian edition: X-ray diffraction in crystals, Fismatgis, Moscow, 1961).
[2] R.W. James, The optical principles of the diffraction of X-rays, London, 1950, chs. 9–10. (Russian edition: Inostrannaja literatura, Moscow, 1950).
[3] B.E. Warren, X-ray Diffraction, Addison Wesley, Reading, 1969, ch. 10.
[4] A.F. Skrishevskii, Structure Analysis of Liquids and Amorphous Bodies, High school, Moscow, 1980 (Russian).
[5] V.I. Korsunsky, J. Struct. Chem. 26 (1985) 75, 208 (N2, Russian, Engl. Trans.).
[6] V.I. Korsunsky, J. Struct. Chem. 26 (1985) 77, 384 (N3, Russian, Engl. Trans.).
[7] M.P. Laurent, J. Biscoe, H.H. Patterson, J. Am. Chem. Soc. 102 (1980) 6575.
[8] (a) R. Serimaa, S. Vahvaselkä, T. Laitalainen, T. Paakkari, A. Oksanen, J. Am. Chem. Soc. 115 (1993) 10036. (b) R. Serimaa, V. Eteläniemi, T. Laitalainen, A. Bienenstock, S. Vahvaselkä, T. Paakkari, Inorg. Chem. 36 (1997) 5574. (c) V. Eteläniemi, R. Serimaa, T. Laitalainen, T. Paakkari, J. Chem. Soc. Dalton Trans. (1998) 3001.
[9] L. Bengtsson-Kloo, M.C. Iapalucci, G. Longoni, S. Ulvenlund, Abstract Book, Sixth International Conference in Chemistry of the Platinum Group Metals, York, 1996, Abs. I.6.
[10] D. Atzei, D. DeFilippo, A. Rossi, R. Caminiti, C. Sadun, Inorg. Chim. Acta 248 (1996) 203.
[11] V.I. Korsunsky, Doklady AN SSSR 291 (1986) 1411.
[12] V.I. Korsunsky, J. Organomet. Chem. 311 (1986) 357.
[13] V.I. Korsunsky, J. Struct. Chem. 28 (1987) 80, 67 (N1, Russian, Engl. Trans.).
[14] E.I. Smyslova, E.G. Perevalova, V.P. Dyadchenko, K.I. Grandberg, Yu. L. Slovokhotov, Yu. T. Struchkov, J. Organomet. Chem. 215 (1981) 269.
[15] L.F. Dahl, E. Ishishi, R.E. Rundle, J. Chem. Phys. 26 (1957) 1750.
[16] P.A. Koz'min, M.D. Surazhskaya, T.B. Larina, Koordinatsionnaja Khimija 5 (1979) 752 (Russian).
[17] V.I. Korsunsky, G.S. Muraveiskaya, V.E. Abashkin, I.G. Fomina, Russ. J. Inorg. Chem. 37 (1992) 2019, 1042 (Russian Engl. Trans.).
[18] P.A. Koz'min, M.D. Surazhskaya, T.B. Larina, Doklady AN SSSR 280 (1985) 929.
[19] D.P. Bancroft, F.A. Cotton, L.R. Falvello, S. Han, W. Schowotzer, Inorg. Chim. Acta 87 (1984) 147.
[20] V.I. Korsunsky, G.N. Kuznetsova, Russ. J. Inorg. Chem. 33 (1988) 1624, 923 (Russian, Engl. Trans.).
[21] M.R. Churchill, B.G. De Boer, Inorg. Chem. 16 (1977) 878.
[22] V.I. Korsunsky, Russ. J. Inorg. Chem. 34 (1989) 139, 77 (Russian, Engl. Trans.).
[23] V.E. Abashkin, I.G. Fomina, V.I. Korsunsky, Koordinatsionnaja Khimija 16 (1990) 979 (Russian).
[24] V.E. Abashkin, I.G. Fomina, V.I. Korsunsky, Koordinatsionnaja Khimija 24 (1998) 123 (Russian).
[25] P.A. Koz'min, V.V. Lapkin, L.K. Shubochkin, M.D. Surazhskaya, E.F. Shubochkina, T.B. Larina, Doklady AN SSSR 286 (1986) 125.
[26] V.I. Korsunsky, T.A. Fomina, N.N. Chalisova, Russ. J. Inorg. Chem. 33 (1988) 2594, 1487 (Russian, Engl. Trans.).
[27] M. Delepine, Compt. Rend. 142 (1906) 631.

[28] M. Ciechanowicz, W.P. Griffith, D. Pawson, A.C. Skapski, M.J. Cleare, J. Chem. Soc. Chem. Commun. (1971) 876.
[29] Le de Boisboudran, Compt. Rend. 96 (1883) 1336.
[30] A.N. Zhilyaev, T.A. Fomina, P.A. Koz'min, T.B. Larina, M.D. Surazhskaya, I.B. Baranovskii, Russ. J. Inorg. Chem. 36 (1991) 400, 222 (Russian, Engl. Trans.).
[31] (a) F.A. Cotton, W. Wang, Inorg. Chem. 21 (1982) 2675. (b) F.A. Cotton, M.W. Extine, L.R. Falvello, D.B. Lewis, G.E. Lewis, C. Murillo, W. Schwotzer, M. Tomas, J.M. Troup, Inorg. Chem. 25 (1986) 3505.
[32] S.I. Ginsburg, M.I. Jusko, L.G. Salskaya, Russ. J. Inorg. Chem. 8 (1963) 839 (Russian).
[33] V.I. Korsunsky, T.A. Fomina, N.N. Chalisova, Russ. J. Inorg. Chem. 35 (1990) 938, 525 (Russian, Engl. Trans.).
[34] V.I. Korsunsky, G.S. Muraveiskaya, V.E. Abashkin, Russ. J. Inorg. Chem. 33 (1988) 669, 374 (Russian, Engl. Trans.).
[35] J.K. Barton, D.J. Szalda, H.N. Rabinowitz, J.V. Waszezak, S.J. Lippard, J. Am. Chem. Soc. 101 (1979) 1434.
[36] M. Peilert, A. Erxleben, B. Lippert, Z. Anorg. Allg. Chem. 622 (1996) 267.
[37] K. Matsumoto, K. Sakai, K. Nishio, Y. Tokisue, R. Ito, T. Nishide, Y. Shichi, J. Am. Chem. Soc. 114 (1992) 8110.
[38] V.I. Korsunsky, V.E. Abashkin, I.G. Fomina, Koordinatsionnaja Khimija 24 (1998) 343 (Russian).
[39] L.M. Epstein, E.S. Shubina, L.N. Saitculova, V.I. Korsunsky, E.I. Smislova, K.I. Grandberg, D.N. Kravtsov, Metalloorgan. Khimija 2 (1989) 1009 (Russian).
[40] E.G. Perevalova, K.I. Grandberg, E.I. Smyslova, L.G. Kuz'mina, V.I. Korsunsky, D.N. Kravtsov, Metalloorgan. Khimija 2 (1989) 1002 (Russian).
[41] A.V. Belyaev, M.A. Fedotov, V.I. Korsunsky, A.B. Venediktov, S.P. Khranenko, Koordinatsionnaja Khimija 10 (1984) 911 (Russian).
[42] V.I. Korsunsky, V.A. Kabayeva, N.L. Kovalenko, Koordinatsionnaja Khimija 17 (1991) 91 (Russian).
[43] H. Barminghansen, B.K. Handa, J. Less-Comm. Metal. (1964) 226.
[44] G. Palinkas, E. Kalman, in: I. Hargittai, W.J. Orville-Thomas (Eds.), Diffraction Studies of Non-Crystalline Substances, Akademy Kiado, Budapest, 1981, p. 293.
[45] V.I. Korsunsky, G.S. Muraveiskaya, A.A. Sidorov, Inorg. Chim. Acta 187 (1991) 23.
[46] V.I. Korsunsky, P.G. Antonov, T.P. Lutsko, Polyhedron 11 (1992) 1403.
[47] J.H. Nelson, N.W. Alcock, Inorg. Chem. 21 (1982) 1196.